Article

Simulation and Optimization Design of SiC-Based PN Betavoltaic Microbattery using Tritium Source

Zhang Lin

School of Electronic and Control Engineering, Chang'an University, Xi'an 710064, China;
zhanglin_dk@chd.edu.cn

Abstract: In this paper, the Monte Carlo method and numerical model are used to build the electrical model of a SiC-based betavoltaic microbattery using a ^{3}H source, and the influences of structural parameters and the surface recombination effect on the output characteristics of the SiC PN battery are simulated. According to Monte Carlo calculations based on the energy spectrum of the ^{3}H source, the ionization energy deposition approaches the exponential distribution along the depth direction, and most of the 22rs are concentrated near the material surface. The ionization energy deposition data is converted into non-equilibrium carrier information for the numerical simulation of the battery's output characteristics. The simulation results show that the conversion efficiency of the battery rises first, and then decreases with the increase of the doping concentration of the N region. This is because the N region-doping affects the depletion region width and the built-in electrical potential at the same time. After considering the surface recombination effect, the conversion efficiency decreased significantly. Thinning the thickness of or moderately reducing the doping concentration of the P region will weaken the surface recombination effect.

1. Introduction

The betavoltaic microbattery is a semiconductor device that utilizes the radiation-voltaic effect of charged particles emitted by radioisotopes to output electric energy. Due to its long life, small size and easy integration, the microbattery has potential applications in many areas, and is considered one of the ideal long-term energy sources for MEMS systems.

Taking into account various factors such as the self-absorption effect of radioisotope sources, the irradiation damage of energy converters and the collection efficiency of ionization energy, low-activity and low-energy β radioisotope sources are mostly taken as energy sources by betavoltaic microbatteries [1–4], such as ^{3}H, ^{63}Ni, ^{33}P, ^{147}Pm and so on. Among them, ^{3}H has a long half-life (12.3 years) and a high specific activity. It is also easily available and inexpensive, and is considered one of the ideal energy sources for betavoltaic microbatteries. The electron energy emitted by ^{3}H is relatively low, the range in the semiconductor material is shallow and the ionization energy can be easily collected. At the same time, the performance is more easily affected by the surface structure and the surface recombination effect of the energy converter.

Since there is currently no commercial software that can directly simulate the radiation-voltaic effect, it has been a hot topic in this field to build an electrical model of the betavoltaic microbattery to guide the optimal design of the energy converter [5–8]. Theoretically, the ionization energy distribution calculated based on the energy spectrum of the radioisotope source is applied to the numerical simulation of the battery's output characteristics, and the output characteristics under different factors (especially considering the complex structure, surface recombination, etc.) are accurately simulated to guide the optimal design of the energy converter, which is an ideal modeling

method. Recently, some related research has been reported [9–11]. However, there are still many problems to be solved, especially the simulation of the ^{3}H betavoltaic microbattery, considering the surface recombination and two-dimensional device structure have not yet been reported.

In order to solve the above problems, the model and optimal design of the ^{3}H SiC-based betavoltaic microbattery are proposed in this paper. The ionization energy deposition of the ^{3}H source is calculated by the Monte Carlo method and applied to the numerical simulation of the output characteristics of the battery, and an optimization scheme is proposed.

2. Monte Carlo Method and Simulation

2.1. Ionization Energy Calculation of Incident Electron

A small part of the electrons emitted by the isotope source are bounced off the surface of the material. The remainder of these enter the material and undergo elastic and inelastic collisions during the advance, and their motion tracks are then changed and energy is lost, until finally they are eventually absorbed or escape from the material. Since the highest energy of the electrons emitted by the ^{3}H source is only 18.6 keV, energy loss modes such as displacement effects can be ignored, and the ionization effect is the main mode of energy loss. In this paper, the following method is used to calculate the ionization energy deposition [11–14], which is often used in this field.

In the calculation, two consecutive elastic collisions of the incident electron are defined as one step, so that the whole motion trajectory of the electron is divided into several motion steps. Each step is composed of several inelastic collision events, and the energy loss in each step is regarded as continuous. The motion distance of each step is determined by the step length taken during the calculation and motion direction of the electron. The motion direction of the electron after each elastic collision is determined by the motion direction, as well as a series of random numbers before the collision.

The energy loss of electron is calculated by the following formula [12]:

$$\frac{dE}{dS} = -\frac{78500\,\rho}{E} \cdot \frac{\overline{Z}}{\overline{A}} \cdot \ln\frac{1.166\,E}{\overline{J}} \tag{1}$$

where ρ is the material density, $\overline{Z}$ is the mean atomic number, $\overline{A}$ is the mean atomic weight and $\overline{J}$ is the mean ionization energy.

After multiple scatterings, the energy of the incident electron is below a given threshold (for example, 50 eV) or escapes from the material, and then the calculation ends.

According to the energy spectrum of the radioisotope source, the above calculation will be repeated a sufficient number of times, in order to obtain the ionization energy deposition in the material.

2.2. Simulation Results and Analysis

By the above method, the ionization energy deposition of the ^{3}H source and the 5.7 keV electron in the SiC material (corresponding to the average electron energy of ^{3}H source) was calculated using Matlab software. It is assumed that the electrons are incident on the material surface vertically in the calculation. The beta energy spectrum of the ^{3}H point source obtained from the icrp 38 report is shown in Figure 1.
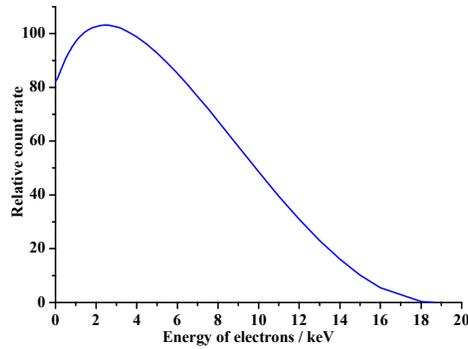
Figure 1. Beta energy spectrum of ³H point source.

The ionization energy distribution of a 5.7 keV electron and ³H source along the material depth direction is shown in Figure 2.
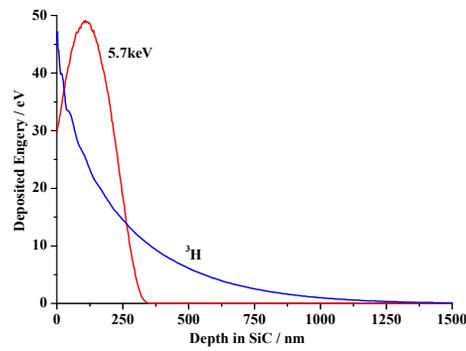

Figure 2. Ionization energy distribution along the material depth direction.

According to Figure 2, the ionization energy of a 5.7 keV electron approaches Gaussian distribution, and the energy is mainly deposited around the peak position. The ionization energy of a ³H source is close to the exponential distribution, and the distribution depth is deeper than that of a 5.7 keV electron. Although the electrons of the ³H source have a range of more than 1.5 μm, the ionization energy is mainly concentrated near the material surface. The energy deposited in 100nm and 313nm accounts for 52.6% and 90% of the total energy, respectively. This is due to the fact that the low-energy electrons in the energy spectrum of a ³H source account for a large proportion (electrons with energy below 5.7 keV are more than 50%).

The above ionization energy distribution characteristics bring some unique problems to the optimization design of betavoltaic microbatteries using a ³H source: (1) If there is an insulating layer or metal layer on the surface of the energy converter, the energy loss of the incident electrons will be relatively high; and (2) the battery output characteristics will be significantly affected by the surface recombination effect.

3. Numerical Model and Simulation

3.1. The Electrical Model of the Betavoltaic Microbattery

The working mechanism of the betavoltaic microbattery is similar to that of the photovoltaic cell. Electron-hole pairs generated by incident particles in the active region of an energy converter are collected to generate output power. According to the drift-diffusion theory, electron-hole pairs generated in the depletion region can be regarded as totally collected. The collection efficiency of electron-hole pairs in the neutral region decreases as the distance from the boundary of the depletion region increases [15]. According to Figure 2, only about a 0.3 μm-wide depletion region is needed to

collect most of the deposited ionization energy. This depletion region width is easily realized in the battery design and process.

Due to its wide bandgap, the wide bandgap semiconductor material represented by SiC can be used to develop the betavoltaic microbattery with a much higher open-circuit voltage than a Si-based battery, which can theoretically get higher conversion efficiency. However, the diffusion length of the SiC is much shorter than that of Si. For isotopes such as [147]Pm, it is difficult to sufficiently collect electron-hole pairs in the depth of material. Due to the shallow range, however, as well as the electrons emitted by a ^{3}H source, the short diffusion length of the SiC material is no longer the main factor affecting the conversion efficiency. The advantages of the SiC material with a wide bandgap will be maximized.

For SiC PN junctions, some material and device characteristics can be described by the following models [11]:

The built-in electrical potential (V_{bi})

$$V_{bi} = \frac{\kappa T}{q} \ln\left(\frac{N_A^+ N_D^+}{n_i^2}\right) \tag{2}$$

where N_A^+, N_D^+ are ionized acceptor and donor impurities, respectively [15, 16], and T is the temperature.

The depletion width (W) can be expressed as:

$$W = \sqrt{\frac{2\varepsilon_s \varepsilon_0}{q}\left(\frac{N_A^+ + N_D^+}{N_A^+ N_D^+}\right)V_{bi}} \tag{3}$$

At room temperature, minority diffusion length of the electron (L_n) and hole (L_p) in SiC

$$L_n = \left(\frac{\kappa T}{q} \cdot \mu_n \cdot \tau_n\right)^{\frac{1}{2}}$$

$$= \left(\frac{\kappa T}{q} \cdot \frac{1020}{1+\left(\frac{N_{doping}}{1.5\times10^{17}}\right)^{0.61}} \cdot \frac{2.5\times10^{-6}}{1+\left(\frac{N_{doping}}{3.0\times10^{17}}\right)^{0.3}}\right)^{\frac{1}{2}}$$

$$L_p = \left(\frac{\kappa T}{q} \cdot \mu_p \cdot \tau_p\right)^{\frac{1}{2}} = \left(\frac{\kappa T}{q} \cdot \frac{112}{1+\left(\frac{N_{doping}}{4\times10^{18}}\right)^{0.4}} \cdot \frac{0.5\times10^{-6}}{1+\left(\frac{N_{doping}}{3.0\times10^{17}}\right)^{0.3}}\right)^{\frac{1}{2}} \tag{4}$$

where μ_n and μ_p are the carrier mobility of the electron and hole, τ_n and τ_p are the minority lifetime of the electron and hole, and N_{doping} is the total doping concentration in SiC.
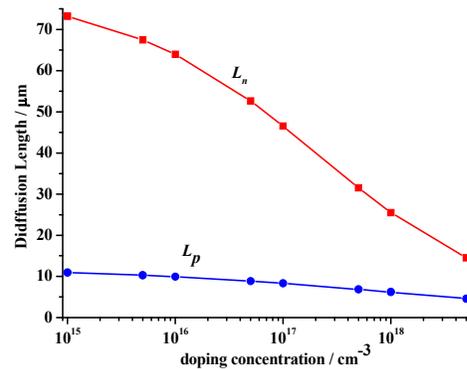
The calculated results of the P[+]N junction (doping concentration of P[+] region is 1×10^{19} cm^{-3}) with different N region doping concentrations is shown in Figure 3:
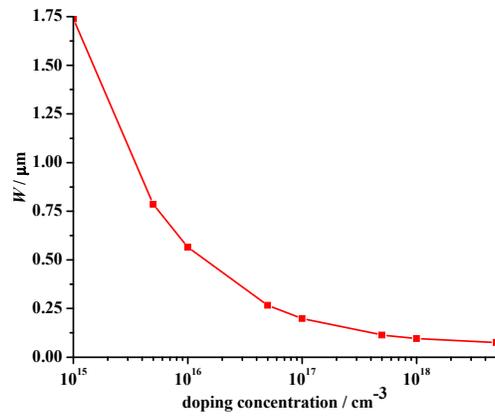
(a)
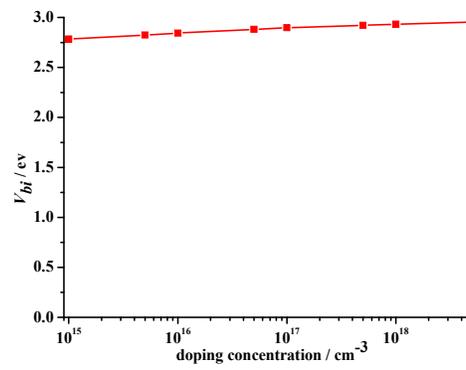
(b)

(c)

Figure 3. *W*, *V$_{bi}$* and diffusion length of SiC P⁺N junction.

W increases with the decrease of the doping concentration of the N region. The wide depletion region can be obtained in the low doping concentration, but it also brings down the Vbi, thereby reducing the open-circuit voltage of the battery. It therefore needs to be taken into account with a compromise in the optimization design of the energy converter.

Even in high doping, the minority diffusion length of SiC is still significantly higher than the electron range of the ³H source. For example, when the doping concentration reaches 1×10^{18} cm⁻³, the L_n and L_p are 25.5 µm and 6.2 µm, respectively. It can be expected that even if some of the electron-hole pairs generate in the neutral region, most of them will also be collected.

Due to the shallow range of the electrons, it is difficult to avoid the carriers loss by the surface recombination. Due to the high hardness and chemical stability of SiC material, the device process is far less mature than that of Si, and there are relatively few research reports. In particular, the surface treatment process and its influence on surface recombination have only few reports, but also have very different test results [17–19]. The influence of the surface recombination effect on the output characteristics of the betavoltaic microbattery is currently limited to some theoretical analysis, which brings difficulties to battery modeling and optimization design.

In theory, in addition to improving the surface treatment process to reduce the surface state, the optimization of the device structure based on the mechanism of surface recombination may also have a role in reducing the negative effect. Therefore, this paper attempts to compare the surface recombination effect on battery performance under different structural parameters, in order to obtain structural optimization results. At present, there is no surface recombination model specific to SiC materials. As a commonly used classic surface recombination model, the following model is adopted for simulation

$$R_{surf}^{SRH} = \frac{np - n_i^2}{(n + n_i)/s_p + (p + n_i)/s_p} \tag{5}$$

where n_i is intrinsic carrier concentration, n and p are the electron and hole concentration respectively, and s_n and s_p are the electron and hole surface recombination velocities respectively. From the formula, it can be seen that the attempt to reduce the doping concentration can reduce the surface recombination rate.

According to the studies based on Si materials, different doping elements and doping concentrations may affect the surface recombination rate [20, 21], but SiC has not been reported. After referring to the reported experimental data, the $s_n = s_p = 1 \times 10^6$ cm/s was taken during simulation in this paper to correspond to the poor condition of the device surface.

3.2. Simulation Results of the Battery Output Characteristics

The ionization energy deposition obtained by the Monte Carlo calculation is converted into the generation rate of electron-hole pairs and mapped to the device grid generated by numerical simulation software, and the radiation-voltaic effect of the device can then be simulated. ISE TCAD is used to simulate the output characteristics of SiC PN betavoltaic microbatteries using a ³H source under the two-dimensional structure of an energy converter, as shown in Figure 4. The intensity of the ³H source is 10 mCi/cm² (3.37 × 10⁻⁷W·cm⁻²), and the electron-hole pair generation energy of the SiC is 10.2 eV (this value is different in different works of literature, and this paper takes a higher value). It is assumed that the electrons emitted from the ³H source incident into the material surface vertically.
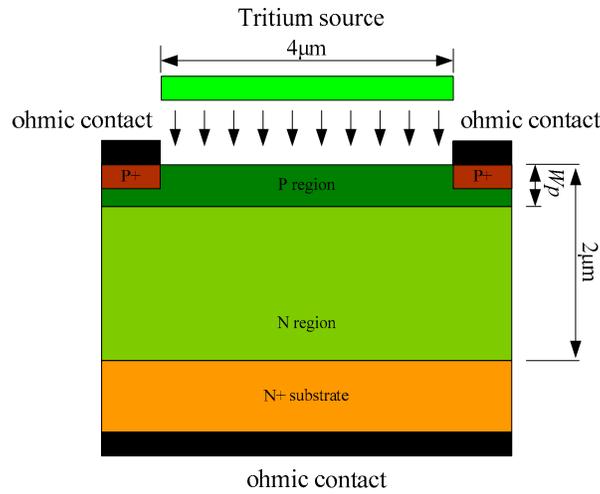
Figure 4. Structure principle diagram of SiC betavoltaic microbattery.

When the thickness of the P region is W_P=0.1μm and the doping concentration of the P region is N_P = 1 × 10^{19} cm^{-3}, the output characteristics and conversion efficiency of the battery with different doping concentrations of the N region (N_N) are shown in Figure 5.
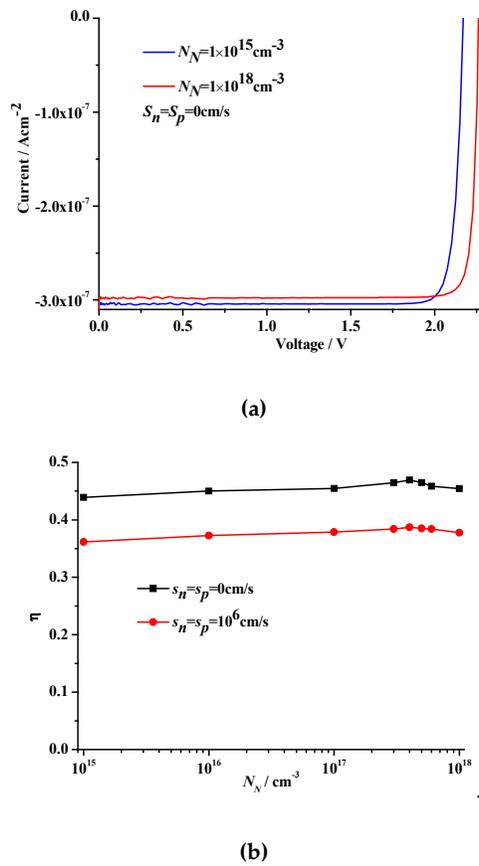

(a)

(b)

Figure 5. Output characteristics (**a**) and conversion efficiency (**b**) of the battery with different N_N.

In Figure 5a, the output characteristics of the battery are not considered the surface recombination effect. As N_N rises, the short-circuit current decreases and the open-circuit voltage rises. The decrease of the short-circuit current is mainly caused by the decrease of the depletion region

width with the increase of the N_N, and the increase of the open-circuit voltage is caused by the increase of the built-in electrical potential.

Simulations show that even if the N_N changes in a large range, the short-circuit current does not change much. This is because the ^{3}H source has a relatively short electron range and the energy is concentrated near the surface. Even if the depletion region width is significantly lower than the electron range, the proportion of electron-hole pairs that fall outside of the depletion region is not high. At the same time, the minority diffusion length is also significantly higher than the distribution depth of electron-hole pairs in the neutral region, so the doping concentration has little influence on the collection efficiency of electron-hole pairs. Changes in short-circuit current and open-circuit voltage affect the conversion efficiency from different trends; the output power reaches a maximum at N_N =4×10^{17}cm^{-3}, corresponding to the conversion efficiency of 46.9%.

After considering the surface recombination effect, the conversion efficiency dropped significantly. When s_n= s_p= 1 × 10^6 cm/s and N_N= 4 × 10^{17} cm^{-3}, the corresponding conversion efficiency is 38.7%, which is significantly lower than that when the surface recombination effect was not considered.

When N_N = 4 × 10^{17}cm^{-3}, the conversion efficiency under different W_P is shown in Figure 6. Regardless of the surface recombination, the conversion efficiency of the battery has little effect when the W_P is changed within the range of 50 nm–200 nm. This is mainly because W_P is far below the L_n of SiC material. Although the electron-hole pairs in the neutral region increase alongside the P region thickness, the number of electron-hole pairs that are recombined is small. After considering the surface combination effect, the conversion efficiency drops significantly with the increase of W_P. This is because as W_P rises, the number of electron-hole pairs participating in the surface recombination increases, and the output characteristics of the battery are affected more by the surface recombination effect.
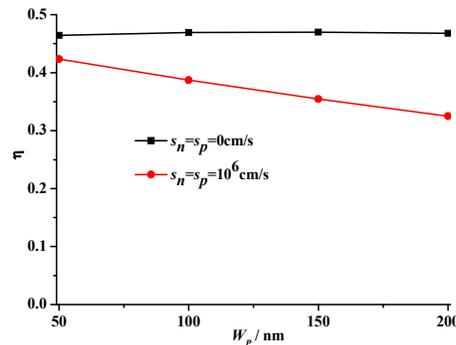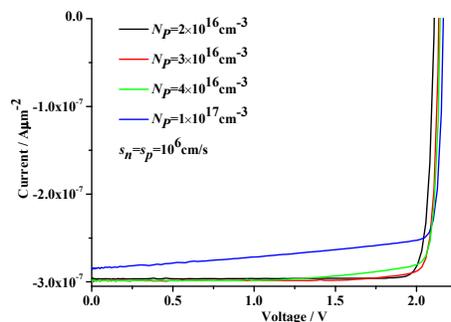

Figure 6. Conversion efficiency of the battery with different W_P.

According to the previous analysis, from the perspective of optimizing the device structure, reducing the doping concentration of the surface region of the energy converter has a certain impact on weakening the surface recombination effect. Figure 7 shows the output characteristics of the battery at different N_P, when W_P= 200 nm and N_N = 4 × 10^{17}cm^{-3}.
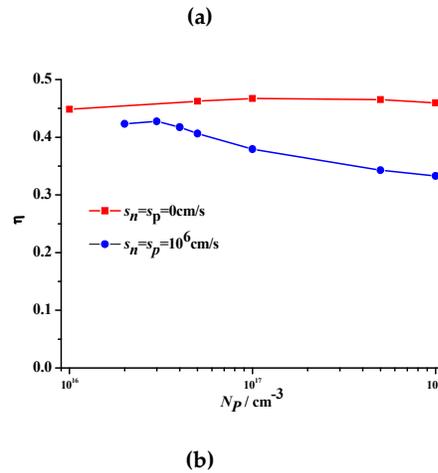
(a)

(b)

Figure 7. Output characteristics (**a**) and conversion efficiency (**b**) of the battery with different N_P.

When the surface recombination is not considered, the conversion efficiency of the battery changes slightly with N_P. This is because the change of N_P mainly affects the built-in electrical potential and the combination of electron-hole pairs in the neutral region. For the study of this paper, however, the impact of these two factors on the conversion efficiency is relatively slight.

After considering the surface recombination effect, the conversion efficiency of the battery increased significantly as the N_P declined. This is due to the gradual depletion near the surface of the energy converter at this time, and the decrease in carrier concentration, which leads to a decrease in the surface recombination rate. When $N_P = 3 \times 10^{16} cm^{-3}$, the conversion efficiency reaches a maximum of 42.7%. When N_P continues to decline, conversion efficiency begins to decrease. This is because the device surface is completely depleted at this time, and the low doping concentration causes the amount of charge in the depletion region of the P region to be too small, which significantly reduces the built-in electrical potential of the junction.

4. Conclusion

Therefore, the surface recombination beyond the recombination in the neutral region becomes an important factor affecting the output characteristics of betavoltaic microbatteries using a ^3H source. According to the simulation, if the surface of the energy converter is in poor condition, the conversion efficiency of the battery will be significantly reduced. For a SiC PN battery, reducing the thickness of the P region or moderately reducing the doping concentration of the P region can effectively weaken the surface recombination effect. In theory, it is the ideal solution to optimize the surface treatment process to reduce the surface recombination rate. However, for SiC material that is not mature enough and treatment that is difficult to process, the research conclusion of this paper has a certain significance for optimizing battery performance and increasing design flexibility. Although the research content of this paper is aimed at SiC-based energy converters and the ^3H source, the research methods can also be applied to other types of microbattery, detectors or sensors based on the radiation-voltaic effect.

In addition, there are also some regrets and aspects to be improved in this paper. The main problem is that a simplified radiation source model is used for simulation, due to the current technical level and the research stage of this paper. Compared with the actual irradiation source, it does not consider the isotropy of the incident particles and the self-absorption effect of the source. The simulation did not take into account the more complex and actual device structure, including the passivation layer on the device surface. Therefore, the conversion efficiency obtained by simulation in this paper is higher than that of the actual situation. It is hoped that with the development of technology, these issues will be paid attention, and focused on in future research.

Conflicts of Interest:　The authors declare no conflict of interest.

References

1. Thomas, C.; Portnoff, S.; Spencer, M.G. High efficiency 4H-SiC betavoltaic power sources using tritium radioisotopes. *Appl. Phys. Lett.* **2016**, *108*, 013505.
2. Qiao, D.Y.; Chen, X.J.; Ren, Y.; Zang, B.; Yuan, W.Z. A nuclear micro-battery based on silicon PIN diode. *Acta Phys. Sin.* **2011**, *60*, 020701.
3. Wang, G.Q.; Li, H.; Lei, Y.S.; Zhao, W.B.; Yang, Y.Q.; Luo, S.Z. Demonstration of Pm-147 GaN betavoltaic cells. *Nucl. Sci. Tech.* **2014**, *25*, 20403–020403.
4. Eiting, C.J.; Krishnamoorthy, V.; Rodgers, S.; George, T.; Robertson, J.D.; Brockman, J. Demonstration of a radiation resistant, high efficiency SiC betavoltaic. *Appl. Phys. Lett.* **2006**, *88*, 064101.
5. Munson, C.E., IV.; Arif, M.; Streque, J.; Belahsene, S.; Martinez, A.; Ramdane, A.; el Gmili, Y.; Salvestrini, J.; Voss, P.L.; Ougazzaden, A. Model of Ni-63 battery with realistic PIN structure. *J. Appl. Phys.* **2015**, *118*, 105101.
6. Sachenko, A.V.; Shkrebtii, A.I.; Korkishko, R.M.; Kostylyov, V.P.; Kulish, M.R.; Sokolovskyi, I.O. Efficiency analysis of betavoltaic elements. *Solid State Electron.* **2015**, *111*, 147–152.
7. Bao, R.; Brand, P.J.; Chrisey, D.B. Betavoltaic Performance of Radiation-Hardened High-Efficiency Si Space Solar Cells. *IEEE Trans. Electron Devices* **2012**, *59*, 1286–1294.
8. Kim, T.; Lee, N.; Jung, H.K.; Kim, J.H. Enhancement of energy performance in betavoltaic cells by optimizing self-absorption of beta particles. *Int. J. Energy Res.* **2016**, *40*, 522–528.
9. Gui, G.; Zhang, K.; Blanchard, J.P.; Ma, Z. Prediction of 4H–SiC betavoltaic microbattery characteristics based on practical Ni-63 sources. *Appl. Radiat. Isot.* **2016**, *107*, 272–277.
10. Zhang, K.; Gui, G.; Pathak, P.; Seo, J.; Blanchard, J.P.; Ma, Z. Quantitative modeling of betavoltaic microbattery performance. *Sens. Actuators A* **2016**, *240,* 131–137.
11. Zhang, L.; Cheng, H.-L.; Hu, X.-C.; Xu, X.B. Model and optimal design of 147Pm SiC-based betavoltaic cell. *Superlattices Microstruct.* **2018**, *123*, 60–70.
12. Love, G.; Cox, M.G.C.; Scott, V.D. A simple Monte Carlo method for simulating electron-solid interactions and its application to electron probe microanalysis. *J. Phys. D Appl. Phys.* **1997**, *10*, 7–23.
13. San, H.; Yao, S.; Wang, X.; Cheng, Z.; Chen, X. Design and simulation of GaN based Schottky betavoltaic nuclear micro-battery. *Appl. Radiat. Isot.* **2013**, *80*, 17–22.
14. Da, K.; Dai, C.-H.; Guo, H. Study of GaN betavoltaic microbattery using Monte Carlo method. *Energy Convert. Microsyst. Technol.* **2013**, *32*, 11–17.
15. Tang, X.B.; Ding, D.; Liu, Y.P.; Chen, D. Optimization design and analysis of Si-63Ni betavoltaic battery. *Sci. China Tech. Sci.* **2012**, *55*, 990–996.
16. Zhang, L.; Yang, F.; Xiao, J.; Gu, W.P.; Qiu, Y.Z. Power characteristics of SiC bipolar-mode JFET. *Acta Phys. Sin.* **2011**, *60*, 107304.
17. Galeckas, A.; Linnros, J.; Frischholz, M.; Grivickas, V. Optical characterization of excess carrier lifetime and surface recombination in 4H/6H–SiC. *Appl. Phys. Lett.* **2001**, *79*, 365–367.
18. Galeckas, A.; Linnros, J.; Frischholz, M.; Rottner, K.; Nordell, N.; Karlsson, S.; Grivickas, V. Investigation of surface recombination and carrier lifetime in 4H/6H-SiC. *Mater. Sci. Eng. B* **1999**, *61–62*, 239–243.
19. Mori, Y.; Kato, M.; Ichimura, M. Estimation of Surface Recombination Velocities for n-Type 4H-SiC Surfaces Treated by Various Processes. *Mater. Sci. Forum* **2014**, *778–780*, 432–435.

20. King, R.R.; Sinton, R.A.; Swanson, R.M. Studies of diffused phosphorus emitters: Saturation current, surface recombination velocity, and quantum efficiency. *IEEE Trans. Electron Devices* **1990**, *37*, 365–371.
21. King, R.R.; Swanson, R.M. Studies of Diffused Boron Emitters: Saturation Current, Bandgap Narrowing, and Surface Recombination Velocity. *IEEE Trans. Electron Devices* **1991**, *38*, 1399–1409.